CR-119844

71- 351

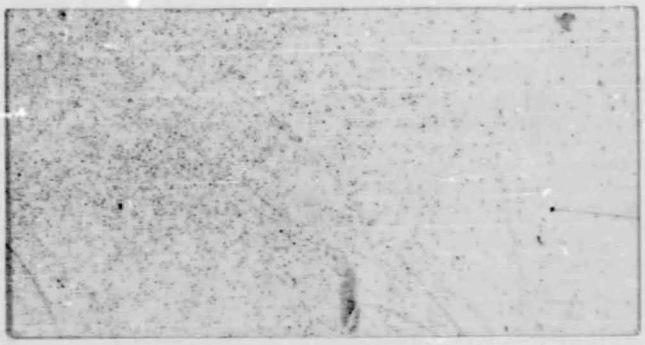

HREC-6189-2
LMSC-HREC D225135-II

LOCKHEED MISSILES & SPACE COMPANY

HUNTSVILLE RESEARCH & ENGINEERING CENTER

HUNTSVILLE RESEARCH PARK

4800 BRADFORD DRIVE, HUNTSVILLE, ALABAMA

STUDY OF THERMAL CONDUCTIVITY REQUIREMENTS

VOL. II

MULTILAYER INSULATION DATA MANUAL – FINAL REPORT

June 1971

Contract NAS8-26189

Prepared for National Aeronautics and Space Administration
Marshall Space Flight Center, Alabama 35812

by

Mark J. O'Neill

A. J. McDanal

APPROVED: Juan K. Lovin

Juan K. Lovin, Supervisor
Thermal Environment Section

George D. Reny

George D. Reny, Manager
Aeromechanics Dept.

George D. Reny
for J.S. Farrior
Resident Director

FOREWORD

This report represents the results of work performed by the Thermal Environment Section of the Aeromechanics Department of Lockheed Missiles & Space Company, Huntsville Research & Engineering Center, for the National Aeronautics and Space Administration, Marshall Space Flight Center, Huntsville, Alabama, under Contract NAS8-26189. The NASA contract monitor was Mr. John Austin of the MSFC Astronautics Laboratory.

The report for "Study of Thermal Conductivity Requirements" consists of three volumes:

Volume I:	Study of Thermal Conductivity Requirements — Multilayer Insulation Thermal Conductivity Test Program — Final Report - NAS8-26189
Volume II:	Study of Thermal Conductivity Requirements — Multilayer Insulation Data Manual — Final Report NAS8-26819
Volume III:	Study of Thermal Conductivity Requirements — Analytical and Experimental Heat Transfer Study of a Venting Cryogen Tank — Final Report - NAS8-26189.

CONTENTS

LIST OF ILLUSTRATIONS

NOMENCLATURE

A	total surface area
K	thermal conductivity
ℓ	layers
m	mass
$\overline{N}$	layer density
t	insulation thickness
W	weight

Greek

$\Delta\overline{N}$	change in layer density
ΔT	change in temperature
ρ	physical density

Subscripts

a	allowable (q_a is allowable heat transfer)
i	inside of insulation
o	outside of insulation
r.s.	reflector shield
s	spacer

Section 1
INTRODUCTION AND SUMMARY

Multilayer insulation (MLI) composites are extremely attractive for space thermal control systems because of their unique thermophysical properties, which include:

- Incomparably low thermal conductivity in vacuum environment
- Very low physical density
- Wide range of temperatures in which the composites can be used
- Low cost and ready availability.

However, the interdependencies between MLI thermophysical properties are complex. For example, the thermal conductivity is strongly dependent on temperature and layer density (the number of composite layers per unit thickness) for all MLI composites. In addition, layer density is extremely dependent on compressive load. Also, the physical density depends directly upon layer density. Analytical techniques are not currently available for adequately predicting the dependencies between thermophysical variables. Therefore, empirical data must be obtained for each MLI composite to specify all interdependencies between thermophysical variables. Only with such data can a thermal design engineer effectively and confidently design MLI space thermal control systems. This report presents experimental data obtained for the following six MLIs:

- Double-aluminized mylar and Tissuglas
- Double-aluminized mylar and Goodyear Aerospace Company (GAC)-9 white foam
- Double-aluminized mylar and dacron net
- Superfloc
- Double-aluminized mylar and Nomex net
- Double-aluminized mylar and Cerex* spunbond nylon.

*Cerex is a registered trademark for a spunbond nylon material manufactured by Monsanto Co.

Experimental data obtained during the test program for these MLI composites include physical density measurements and the response of each composite to mechanical loading. In addition, using the latest design in Lockheed-Huntsville's electrical cylindrical calorimeter, temperature and layer density dependent thermal conductivity data were obtained. The range of test temperatures was -200 to +200°F and the layer density range included all practical values of layer density.

A summary of the data presented in this report is outlined in Chart 1.

Type of Data	Table	Figure	Page
Density	1-6		4-6
		1	7
Compression	7-12		10-12
		3-8	13-18
Thermal	13-18		22-27
		9-20	28-39

Chart 1 - Presentation of Data

Chart 2 summarizes the source and average thickness for each material tested. Double aluminized mylar (DAM) was chosen as the reflective shield to be used with the six spacers because of its extremely good thermal radiation properties.

Material	Source	Nominal Thickness (mil)
Double-aluminized mylar	NRC	0.25
Tissuglas	Pallflex, Inc.	0.6
GAC-9 white foam	Goodyear Aerospace Corp.	20.0
Dacron net (B-4A)	Stern and Stern Textiles	1.2
Superfloc	General Dynamics/Convair Div.	5.0 (flock)
Nomex net	Stern and Stern Textiles	7.0
Cerex spunbond nylon	Monsanto	5.0

Chart 2 - Test Materials

Semiempirical correlations were developed to fit the thermal data and are presented in Section 5.

Section 2
DENSITY DATA

The physical density for an MLI composite is obtained by weighing several 10 x 10-inch samples of the reflector shield and the spacer. From this, an average mass of one 10 x 10 inch sample of the reflector shield and spacer is found. These values are substituted into the following equation

$$\rho = \frac{(\bar{N} + 1)\, m_{r.s.} + (\bar{N})\, m_s}{\text{Area}}$$

where

$m_{r.s.}$ = average mass of one 10 x 10-inch reflective shield

m_s = average mass of one 10 x 10-inch spacer

Area = 100 in^2

$\bar{N}$ = layer density in layers/in.

Tables 1 through 6 present density data for the six MLI materials under study. Figure 1 presents the same data in graphical form.

2.1 DENSITY DATA TABLES

Table 1

DENSITY DATA FOR DAM/TISSUGLAS

Layer Density $\bar{N}$ (layers/in)	Physical Density ρ (lbm/ft^3)	Physical Density Equation
120	2.79	$\rho = 0.0226\ \bar{N} + 0.0212$
160	3.69	
200	4.60	

Table 2

DENSITY DATA FOR DAM/GAC-9

Layer Density $\bar{N}$ (layers/in)	Physical Density ρ (lbm/ft^3)	Physical Density Equation
30	1.78	$\rho = 0.0587\ \bar{N} + 0.0212$
40	2.37	
50	2.96	

Table 3
DENSITY DATA FOR DAM/DACRON NET

Layer Density $\bar{N}$ (layers/in)	Physical Density ρ (lbm/ft^3)	Physical Density Equation
120	4.55	$\rho = 0.0377\ \bar{N} + 0.0212$
160	6.05	
200	7.56	

Table 4
DENSITY DATA FOR SUPERFLOC

Layer Density $\bar{N}$ (layers/in)	Physical Density ρ (lbm/ft^3)	Physical Density Equation
80	1.89	$\rho = 0.0236\ \bar{N}$
160	3.78	
200	4.72	

Table 5

DENSITY DATA FOR DAM/NOMEX NET

Layer Density $\bar{N}$ (layers/in)	Physical Density ρ (lbm/ft^3)	Physical Density Equation
65	5.76	$\rho = 0.0883\ \bar{N} + 0.0212$
80	7.09	
95	8.41	

Table 6

DENSITY DATA FOR DAM/CEREX

Layer Density $\bar{N}$ (layers/in)	Physical Density ρ (lbm/ft^3)	Physical Density Equation
75	3.61	$\rho = 0.0479\ \bar{N} + 0.0212$
100	4.81	
150	7.21	

2.2 DENSITY DATA FIGURE

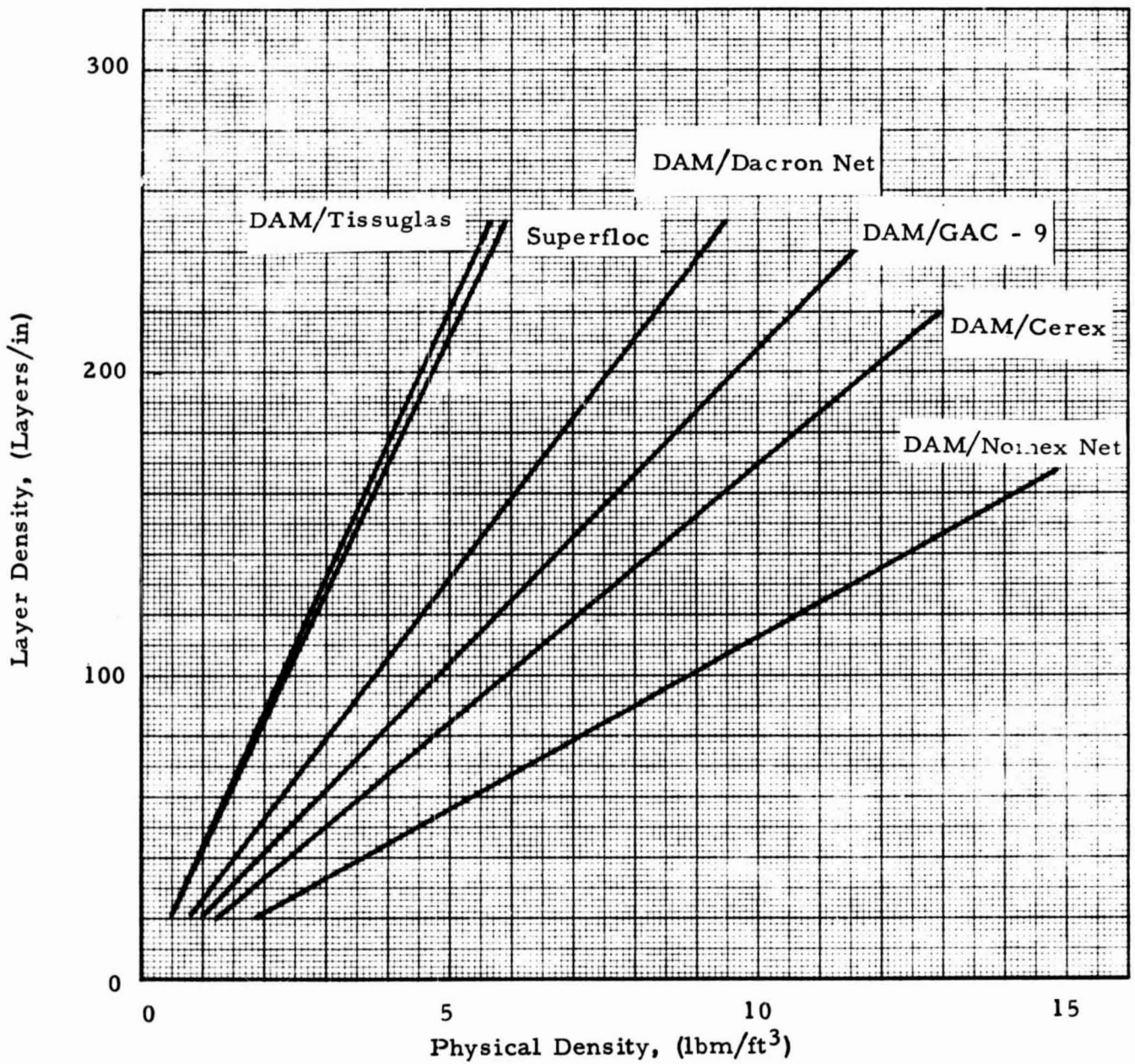

Fig. 1 - Density Data for MLI Composites

Section 3
COMPRESSION DATA

Compression tests for all MLI materials under consideration are performed using the apparatus in Fig. 2. Layers of material 10 in. x 10 in. are cut for each sample. The stacked layers of insulation composite are tested unloaded (Fig. 2a) and loaded with plates of known weights (Fig. 2b). Five thickness measurements are made for each load level; one two inches in from each side and one at the center. These five readings are averaged, and the plate thickness is subtracted to arrive at the stack thickness. This thickness, along with the known number of layers, establishes the layer density. A more complete description of the compression test is given in Ref. 1.*

Compression data are presented for each of the insulations tested in Tables 7 through 12. The number of layers used in each test is indicated in the tables. One layer represents one reflector shield and one spacer (where spacers are used). These data are also presented in graphical form in Figs. 3 through 8.

*Volume I of this document.

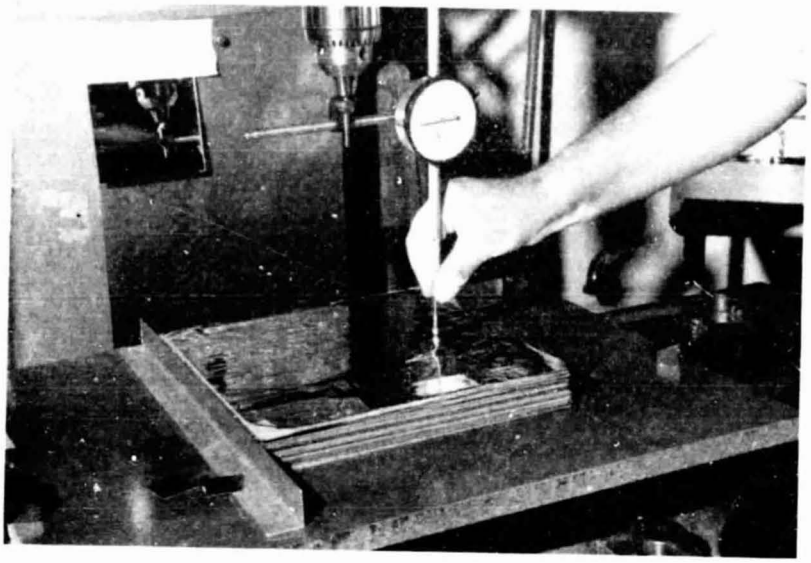

a. Unloaded

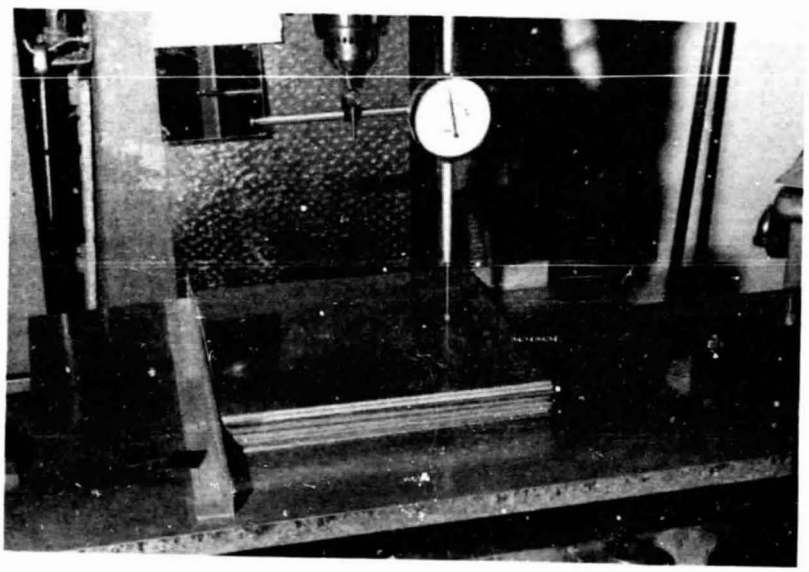

b. Loaded

Fig. 2 - Compression Test Apparatus

3.1 COMPRESSION DATA TABLES

Table 7

COMPRESSION DATA FOR DAM/TISSUGLAS

Number of Layers	Layer Density (Layers/in)	Mechanical Load (lb/in^2)
90	149	0.00054
90	183	0.00162
90	235	0.00668
90	275	0.0258
90	351	0.113

Table 8

COMPRESSION DATA FOR DAM/GAC-9

Number of Layers	Layer Density (Layers/in)	Mechanical Load (lb/in^2)
15	32.1	0.000261
15	33.0	0.00134
38	33.8	0.000652
38	34.1	0.00173
38	37.4	0.00679
38	39.3	0.0259
38	41.9	0.107

Table 9

COMPRESSION DATA FOR DAM/DACRON NET

Number of Layers	Layer Density (Layers/in)	Mechanical Load (lb/in^2)
25	83.3	0.00272
50	88.8	0.000545
50	109.2	0.00163
50	150.1	0.00669
50	200.8	0.0258
50	301.2	0.107

Table 10

COMPRESSION DATA FOR SUPERFLOC

Number of Layers	Layer Density (Layers/in)	Mechanical Load (lb/in^2)
25	31.9	0.000171
25	44.5	0.00125
50	35.4	0.000342
50	56.0	0.00142
50	109.2	0.00648
50	208.3	0.0256
50	568.2	0.106

Table 11

COMPRESSION DATA FOR DAM/NOMEX NET

Number of Layers	Layer Density (Layers/in)	Mechanical Load (lb/in^2)
25	55.9	0.000645
25	65.1	0.00172
50	62.1	0.00128
50	63.8	0.00236
50	73.0	0.00742
50	83.2	0.0266
50	114.4	0.107

Table 12

COMPRESSION DATA FOR DAM/CEREX

Number of Layers	Layer Density (Layers/in)	Mechanical Load (lb/in^2)
25	81.2	0.000352
25	120.8	0.00143
50	93.6	0.000699
50	122.2	0.00178
50	167.8	0.00684
50	196.9	0.0260
50	237.0	0.107

3.2 COMPRESSION DATA FIGURES

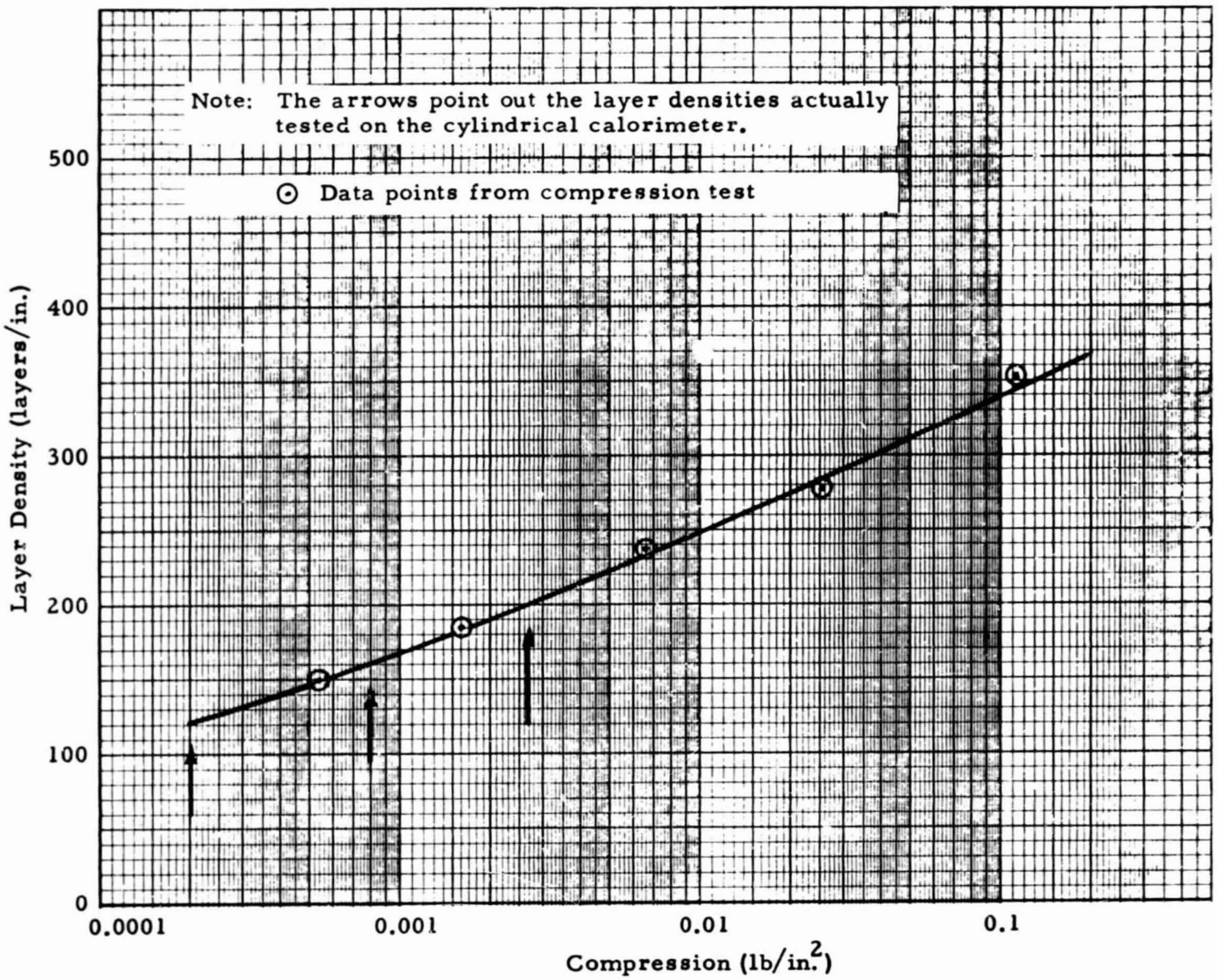

Fig. 3 - Compressibility Data for DAM/Tissuglas

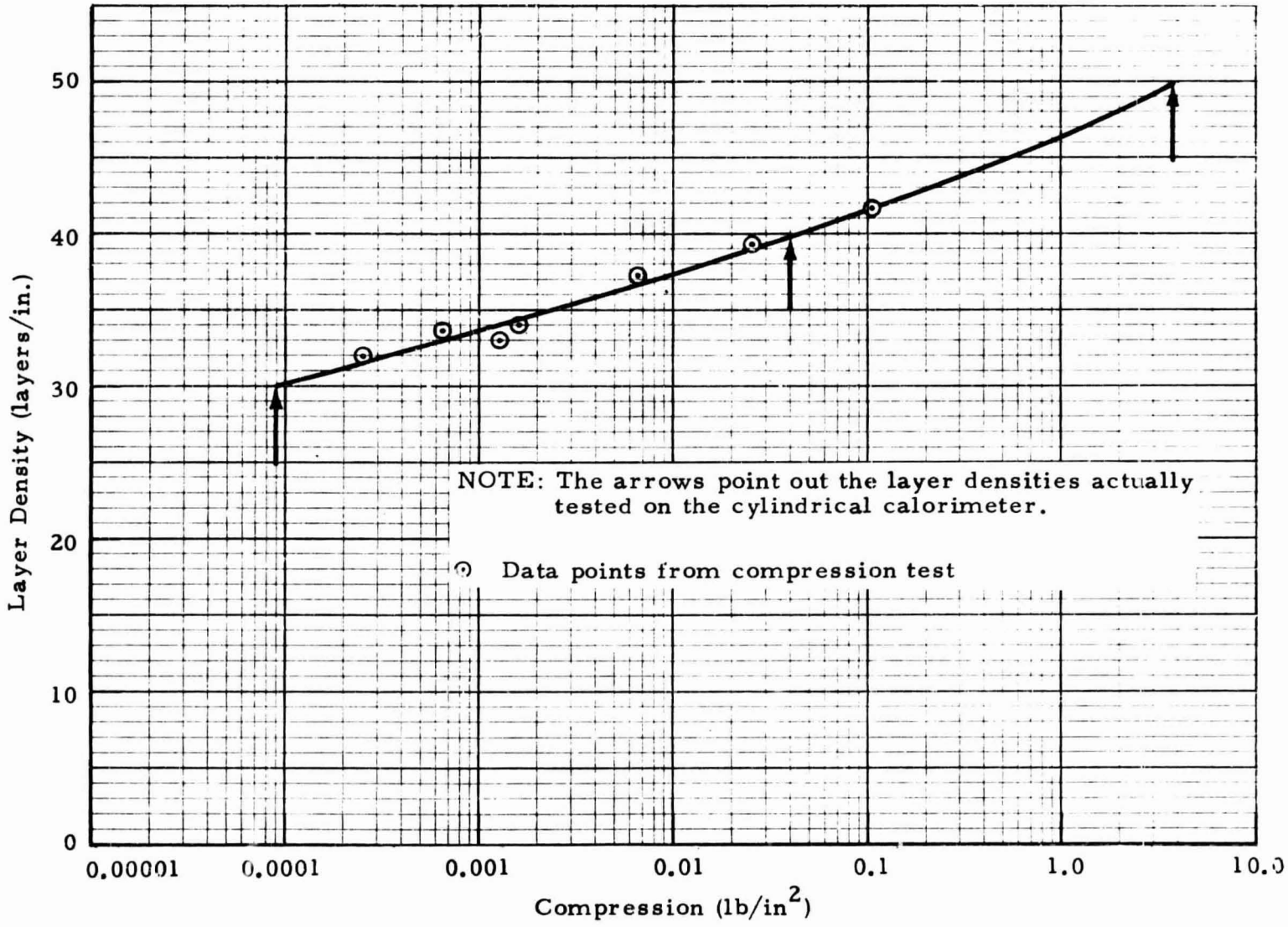

Fig. 4 - Compressibility Data for DAM/GAC-9

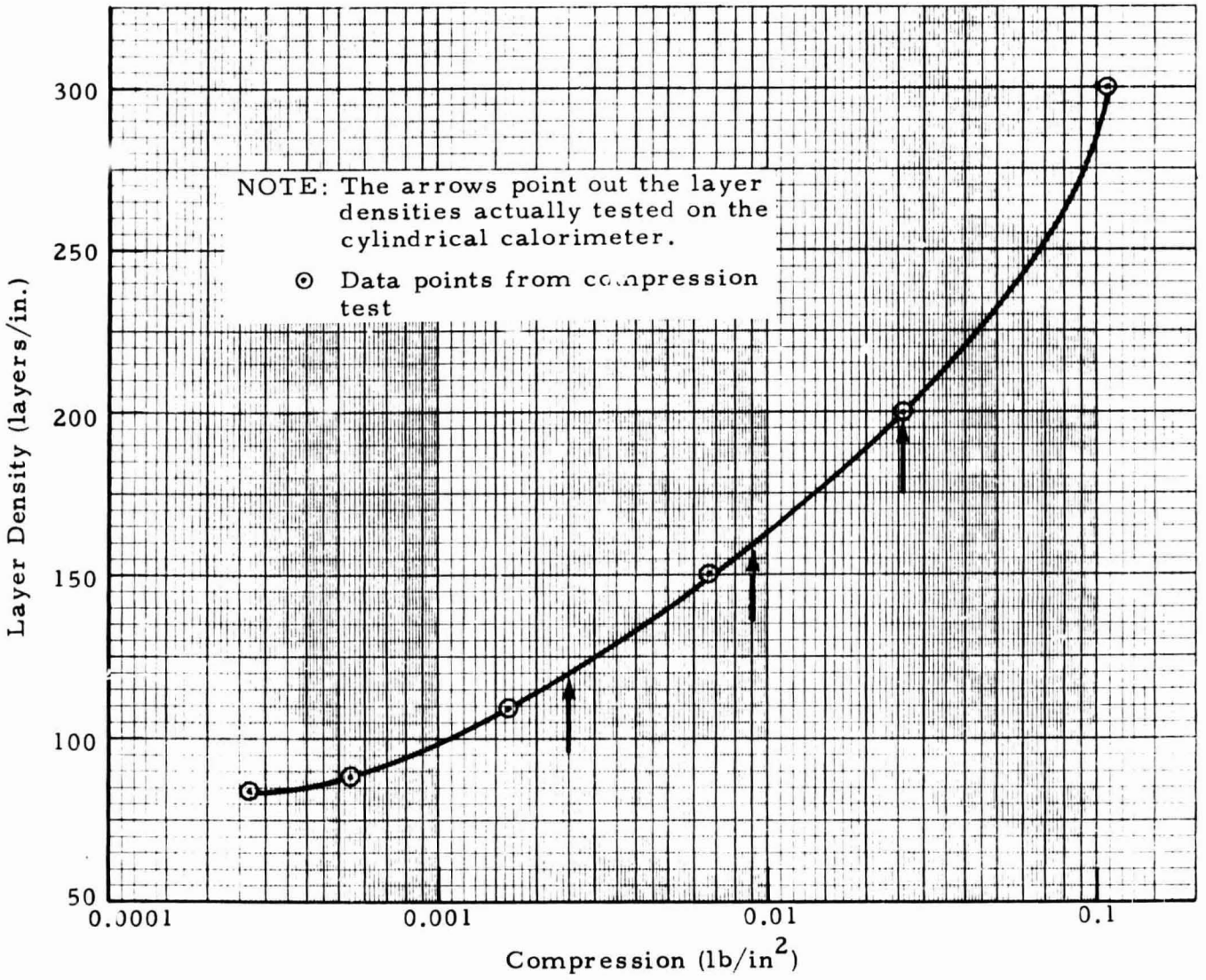

Fig. 5 - Compressibility Data for DAM/Dacron Net

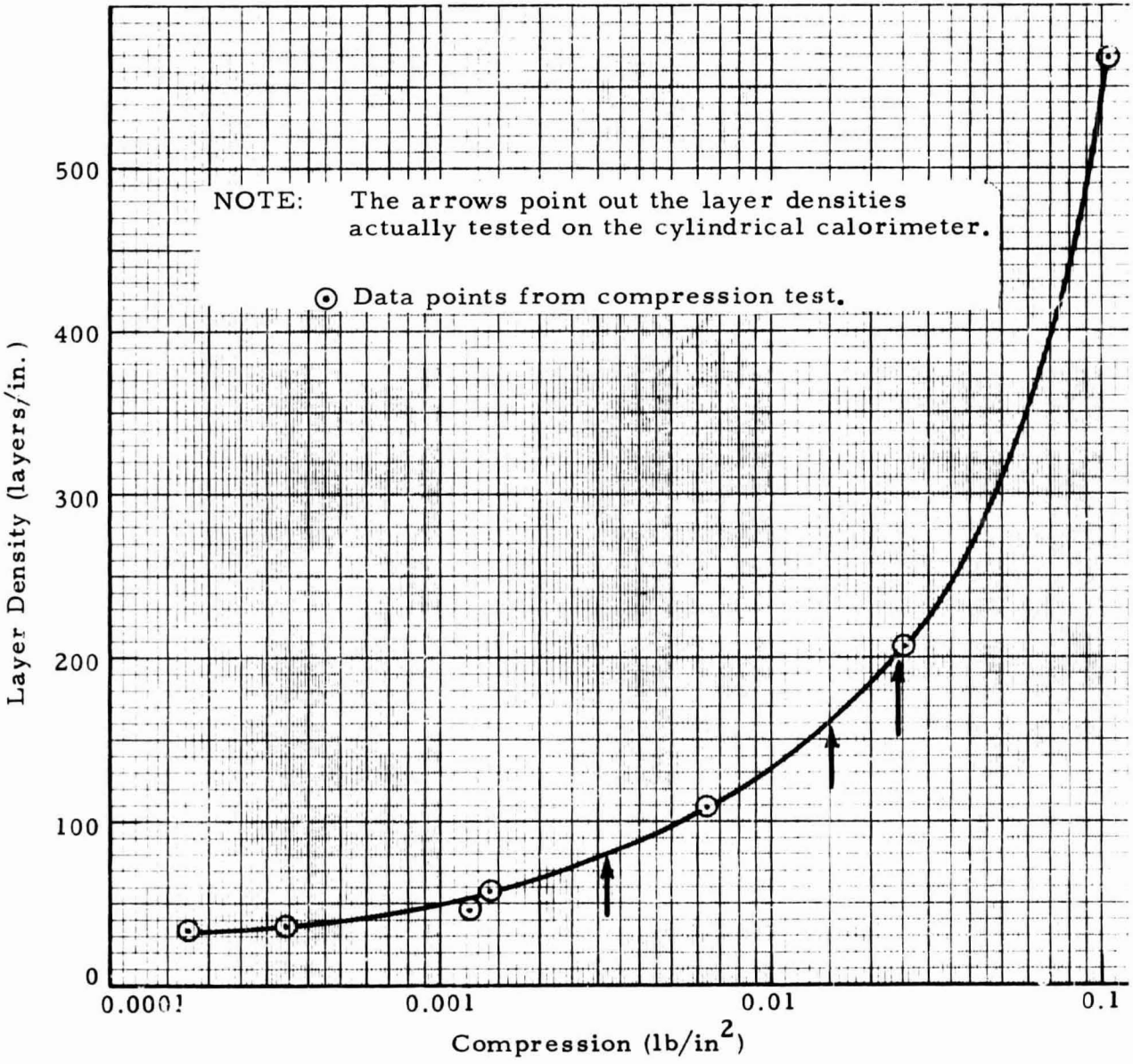

Fig. 6 - Compressibility Data for Superfloc

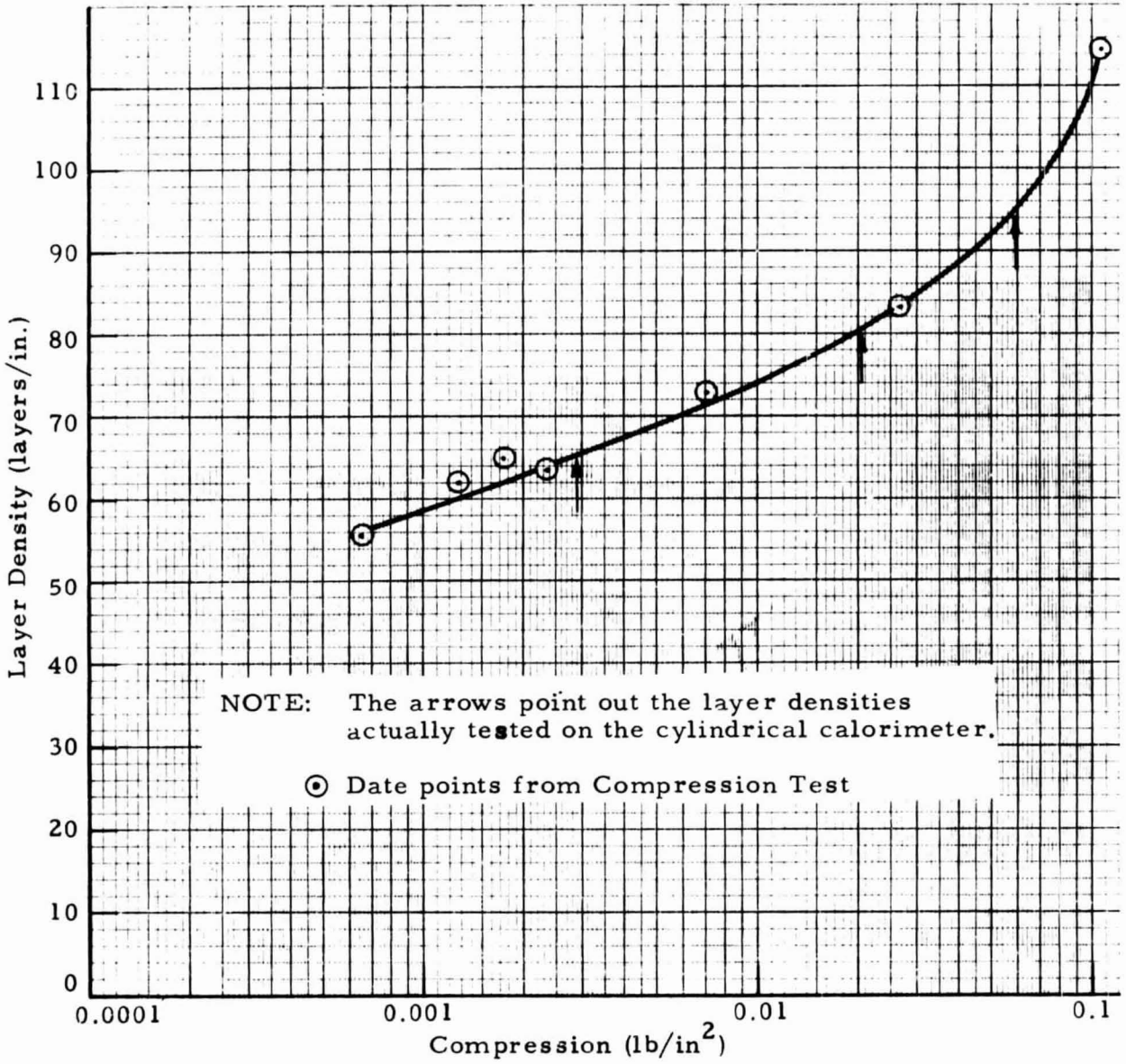

Fig. 7 - Compressibility Data for DAM/Nomex Net

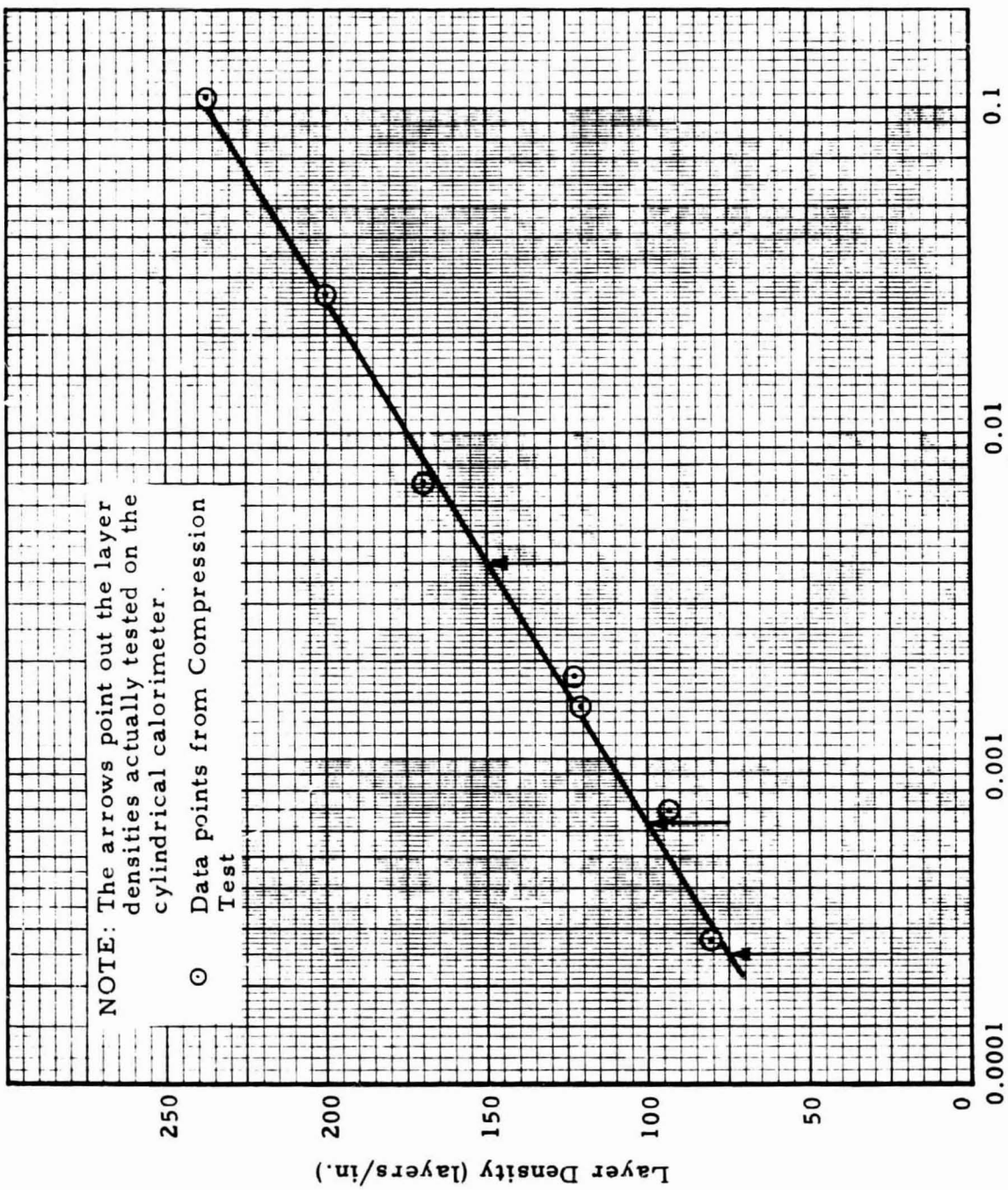

Fig. 8 - Compressibility Data for DAM/Cerex

Section 4
THERMAL DATA AND ERROR ANALYSIS

Thermal conductivity tests were performed on six MLI composites using the Lockheed-Huntsville electrical cylindrical calorimeter. A detailed description of the cylindrical calorimeter, method of specimen preparation, and thermal conductivity testing are presented in Ref. 1*. Thermal conductivity testing was conducted over a range of temperatures from -200 to +200°F, and over a range of layer densities from a minimum practical density to a highly compressed layer density. The actual data points obtained during the test program are presented in Section 4.1.

Thermal conductivity data obtained from the calorimeter are verified by error analysis for each data point obtained. To determine the error in thermal conductivity, the error introduced by heat storage, longitudinal heat loss and physical measurements is determined. Reference 2** gives a precise treatment of the error analysis, and results of the analysis are presented in Tables 13 through 18 as a ± % probable error. An average probable error of ± 2.10% was found for all data points obtained during the test program.

In Sections 4.2 (Figs. 9 through 14) and 4.3 (Figs. 15 through 20) of this report, thermal conductivity and density times thermal conductivity are presented as a function of temperature and layer density in carpet plot form for all multilayer insulations tested.

---

*Volume I of this document

**Hale, D. V., and M. J. O'Neill, "Study of Thermal Conductivity Requirements," LMSC-HREC D162128, Lockheed Missiles & Space Company, Huntsville, Ala., February 1970.

The presentation of MLI thermal conductivity data in carpet plot form is an innovation developed during this study. Since MLI thermal conductivity is a function of the two independent variables, temperature and layer density, the data can be presented in carpet plot form which allows exact double interpolation to determine the value of conductivity for any set of $(T, \bar{N})$ within the ranges of the data. Presentation of the data in family-of-curves form would not allow such double interpolation. For a detailed description and example of double interpolation, the reader should consult Appendix A. Density times thermal conductivity (ρK) data are also presented in carpet plot form.

Density times thermal conductivity data are presented due to the extreme importance of the ρK product in multilayer insulation design work for weight-limited applications. Presentation of data in ρK form is duly justified by the following derivation.

For most weight limited MLI system applications the following variables are fixed:

$\Delta T = T_i - T_o$ (Temperature differential through the insulation)

A = Total surface area

q_a = Allowable heat transfer.

The conduction equation for this process is

$$q_a = \frac{KA\Delta T}{t} \tag{1}$$

where t is the insulation thickness. Solving this equation for t gives

$$t = \frac{KA\Delta T}{q_a} \ . \tag{2}$$

The weight of the MLI system is:

$$W = \rho A t \tag{3}$$

where W is the weight and ρ is the physical density of the MLI. Substituting Eq. (2) above into this equation yields:

$$W = \rho A \left[\frac{KA\Delta T}{q_a}\right]. \tag{4}$$

Rearranging:

$$W = \rho K \left[\frac{A^2\Delta T}{q_a}\right]. \tag{5}$$

Since the term within the brackets is a constant quantity,

$$W = \rho K \times \text{constant} \tag{6}$$

and ρK is seen to be the parameter to minimize for weight-limited applications.

Figures 15 through 20 present density x thermal conductivity product in carpet plot form for the six MLI materials tested.

4.1 THERMAL DATA TABLES

Table 13

THERMAL DATA FOR DAM/TISSUGLAS

Layer Density $\bar{N}$ (layers/in)	Chamber Pressure (torr)	ΔT (^{o}F)	Mean Temperature (^{o}F)	Thermal Conductivity ($K \times 10^{5}$) (Btu/hr-ft-^{o}F)	Density x Thermal Conductivity ($\rho K \times 10^{5}$) (Btu/hr-ft-^{o}F) x (lbm/ft^{3})	Probable Error $\pm$ (%)
120	7.0×10^{-7}	40.2	-198.1	0.77	2.13	1.02
120	3.4×10^{-7}	35.0	- 60.5	3.16	8.72	1.15
120	4.0×10^{-7}	31.9	66.9	12.60	34.78	1.32
120	5.2×10^{-6}	29.0	191.1	29.50	81.42	1.40
160	1.0×10^{-7}	38.2	-199.6	1.41	5.19	1.03
160	9.4×10^{-8}	42.1	- 53.4	3.62	13.32	0.896
160	1.2×10^{-7}	38.5	68.7	12.04	44.31	1.19
160	1.9×10^{-6}	36.5	195.0	20.95	77.10	1.90
200	9.0×10^{-8}	33.6	-198.2	2.33	10.72	1.11
200	9.0×10^{-8}	46.2	- 72.6	2.68	12.33	1.16
200	2.2×10^{-7}	41.1	94.8	5.65	25.99	1.59
200	4.0×10^{-6}	43.8	200.1	19.65	90.39	3.16

Table 14

THERMAL DATA FOR DAM/GAC-9

Layer Density $\bar{N}$ (layers/in)	Chamber Pressure (Torr)	ΔT (^{o}F)	Mean Temperature (^{o}F)	Thermal Conductivity ($K \times 10^{5}$) (Btu/hr-ft-^{o}F)	Density x Thermal Conductivity ($\rho K \times 10^{5}$) (Btu/hr-ft-^{o}F) (lbm/ft^{3})	Probable Error $\pm$(%)
30	2.0×10^{-7}	33.7	-208.6	0.96	1.71	1.64
30	1.5×10^{-7}	26.6	- 63.6	2.66	4.81	1.83
30	2.2×10^{-7}	17.6	86.5	5.95	10.51	1.91
30	9.8×10^{-7}	32.9	208.4	15.11	26.92	2.26
40	3.0×10^{-7}	15.2	-195.1	1.88	4.44	2.25
40	4.0×10^{-7}	39.2	- 58.4	3.93	9.30	2.36
40	6.0×10^{-7}	15.4	89.7	6.08	14.39	2.25
40	1.1×10^{-6}	22.1	198.2	14.15	33.51	2.64
50	2.4×10^{-7}	24.0	-190.5	2.02	5.98	2.82
50	4.0×10^{-7}	32.6	- 59.3	3.69	10.91	2.87
50	4.5×10^{-7}	16.1	84.4	6.84	20.20	2.85
50	6.0×10^{-7}	30.5	194.6	13.31	39.32	2.90

Table 15

THERMAL DATA FOR DAM/DACRON NET

Layer Density $\bar{N}$ (Layers/in)	Chamber Pressure (Torr)	ΔT (^{o}F)	Mean Temperature (^{o}F)	Thermal Conductivity ($K \times 10^{5}$) (Btu/hr-ft-^{o}F)	Density x Thermal Conductivity ($\rho K \times 10^{5}$) (Btu/hr-ft-^{o}F) (lbm/ft^{3})	Probable Error $\pm$ (%)
120	6.0×10^{-7}	20.6	-193.0	1.36	5.14	1.12
120	8.0×10^{-7}	34.9	- 56.2	1.95	7.37	1.27
120	6.0×10^{-7}	23.4	86.9	8.62	32.65	1.90
120	8.0×10^{-7}	38.8	198.9	20.18	76.44	2.92
160	6.0×10^{-7}	39.5	-200.8	1.77	10.71	1.54
160	3.0×10^{-7}	49.0	- 61.5	2.65	16.02	1.88
160	3.5×10^{-7}	34.9	97.1	5.23	31.66	1.64
160	4.5×10^{-7}	38.3	198.8	9.92	60.03	1.74
200	8.0×10^{-8}	29.4	-197.7	1.96	14.83	1.62
200	1.5×10^{-7}	23.5	- 62.8	2.77	20.92	1.97
200	2.0×10^{-7}	17.0	87.8	4.53	34.22	1.95
200	7.0×10^{-7}	33.6	198.5	10.15	76.70	1.83

Table 16

THERMAL DATA FOR SUPERFLOC

Layer Density $\bar{N}$ (Layers/in)	Chamber Pressure (Torr)	ΔT (^{o}F)	Mean Temperature (^{o}F)	Thermal Conductivity ($K \times 10^{5}$) (Btu/hr-ft-^{o}F)	Density x Thermal Conductivity ($\rho K \times 10^{5}$) (Btu/hr-ft-^{o}F) (lbm/ft^{3})	Probable Error $\pm$ (%)
80	2.0×10^{-9}	47.0	-202.3	1.93	3.65	0.924
80	1.0×10^{-8}	50.9	- 66.1	5.42	10.24	6.51
80	6.2×10^{-7}	26.1	96.8	10.24	19.36	0.988
80	5.2×10^{-7}	36.7	199.0	17.07	32.26	7.53
160	1.5×10^{-8}	24.8	-194.6	2.78	10.51	1.51
160	2.4×10^{-8}	49.8	- 68.3	5.13	19.37	1.53
160	3.0×10^{-7}	32.0	94.9	8.72	32.93	1.52
160	4.0×10^{-7}	34.5	197.8	11.31	42.73	1.69
200	3.0×10^{-8}	21.4	-190.5	2.43	11.48	1.85
200	1.6×10^{-7}	37.4	- 58.4	6.65	31.41	1.86
200	3.0×10^{-7}	26.4	96.9	10.01	47.29	1.86
200	3.3×10^{-7}	36.5	198.2	15.03	71.00	2.05

Table 17

THERMAL DATA FOR DAM/NOMEX NET

Layer Density $\overline{N}$ (Layers/in)	Chamber Pressure (Torr)	ΔT (^{o}F)	Mean Temperature (^{o}F)	Thermal Conductivity ($K \times 10^5$) (Btu/hr-ft-^{o}F)	Density x Thermal Conductivity ($\rho K \times 10^5$) (Btu/hr-ft-^{o}F) (lbm/ft^3)	Probable Error $\pm$ (%)
65	1.5×10^{-5}	39.9	-190.6	0.81	4.64	1.22
65	1.0×10^{-6}	59.9	- 67.2	2.68	15.42	1.38
65	$\leq$* 8.0×10^{-6}	24.4	88.6	10.72	61.75	6.27
65	5.5×10^{-7}	36.9	199.2	16.29	93.82	4.57
80	1.0×10^{-8}	45.1	-199.0	1.60	11.35	1.33
80	1.8×10^{-8}	56.4	- 62.0	3.19	22.59	2.15
80	1.8×10^{-8}	32.8	99.5	6.76	47.89	2.28
80	1.0×10^{-7}	35.4	196.8	14.52	102.81	1.55
95	8.0×10^{-6}	35.3	-197.1	2.79	23.46	3.28
95	2.4×10^{-8}	51.0	- 64.9	4.56	38.34	1.57
95	4.0×10^{-7}	34.0	99.4	10.12	85.12	1.51
95	2.0×10^{-7}	32.7	196.8	15.56	130.77	1.57

*Exact pressure reading was not obtained due to faulty pressure gage.

Table 18

THERMAL DATA FOR DAM/CEREX

Layer Density $\bar{N}$ (layers/in)	Chamber Pressure (torr)	ΔT (^{o}F)	Mean Temperature (^{o}F)	Thermal Conductivity ($K \times 10^{5}$) (Btu/hr-ft-^{o}F)	Density x Thermal Conductivity ($\rho K \times 10^{5}$) (Btu/hr-ft-^{o}F) x (lbm/ft^{3})	Probable Error $\pm$(%)
75	3.5×10^{-6}	41.0	-190.1	2.29	8.27	1.45
75	5.6×10^{-6}	50.3	0.4	4.42	15.97	1.63
75	6.0×10^{-6}	36.9	198.8	13.03	47.07	1.87
100	1.4×10^{-8}	40.4	-186.8	3.10	14.91	1.91
100	1.0×10^{-7}	43.9	7.2	5.11	24.58	1.90
100	2.4×10^{-6}	29.7	194.0	18.49	88.92	2.23
150	*$\leq 8.0 \times 10^{-6}$	32.2	-182.1	4.21	30.33	2.78
150	*$\leq 8.0 \times 10^{-6}$	35.6	- 17.8	7.07	50.93	2.78
150	*$\leq 8.0 \times 10^{-6}$	27.5	198.9	23.54	169.56	2.86

*Exact pressure reading was not obtained due to faulty pressure gage.

4.2 THERMAL CONDUCTIVITY DATA FIGURES

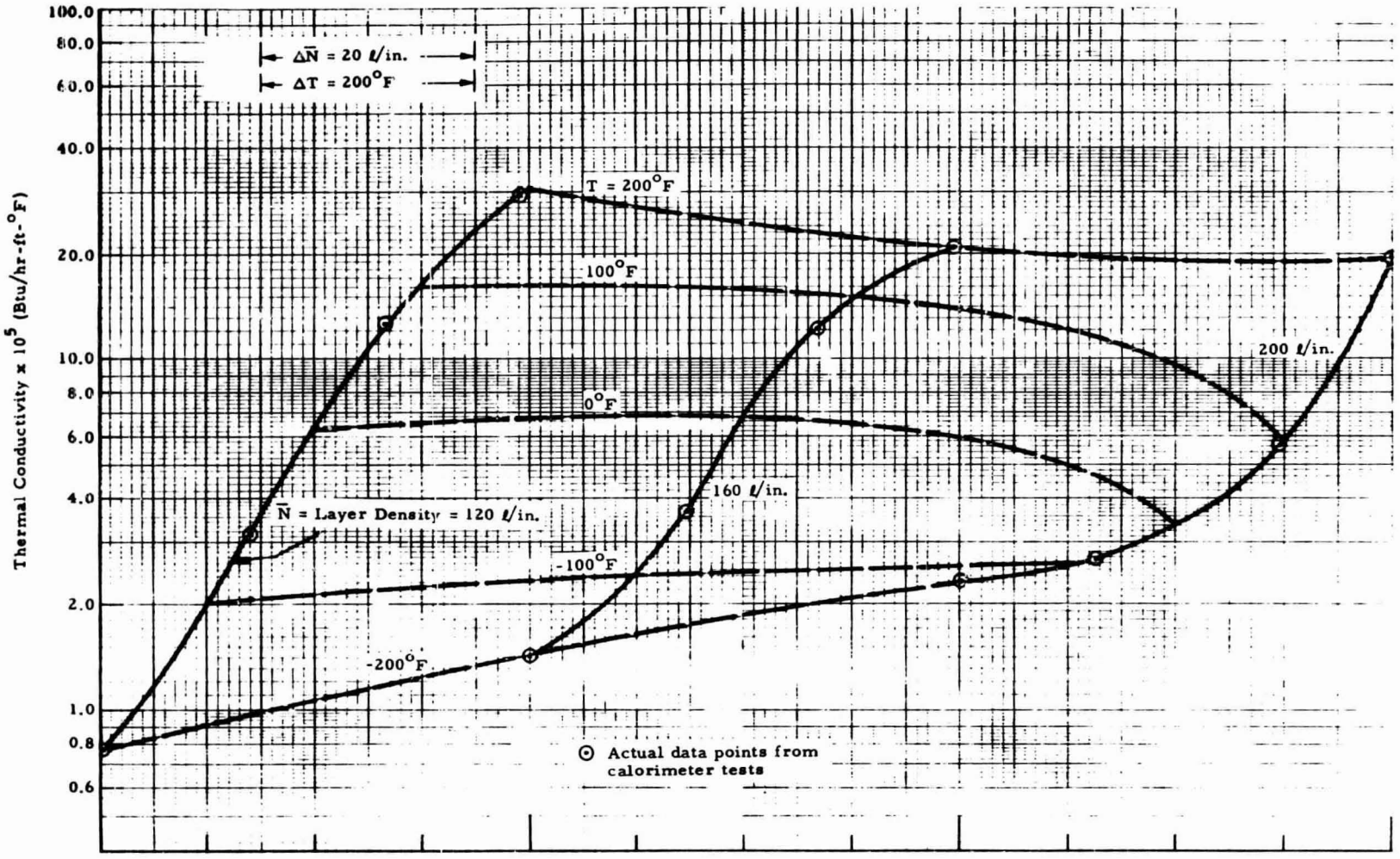

Fig. 9 - Thermal Conductivity Carpet Plot for DAM/Tissuglas

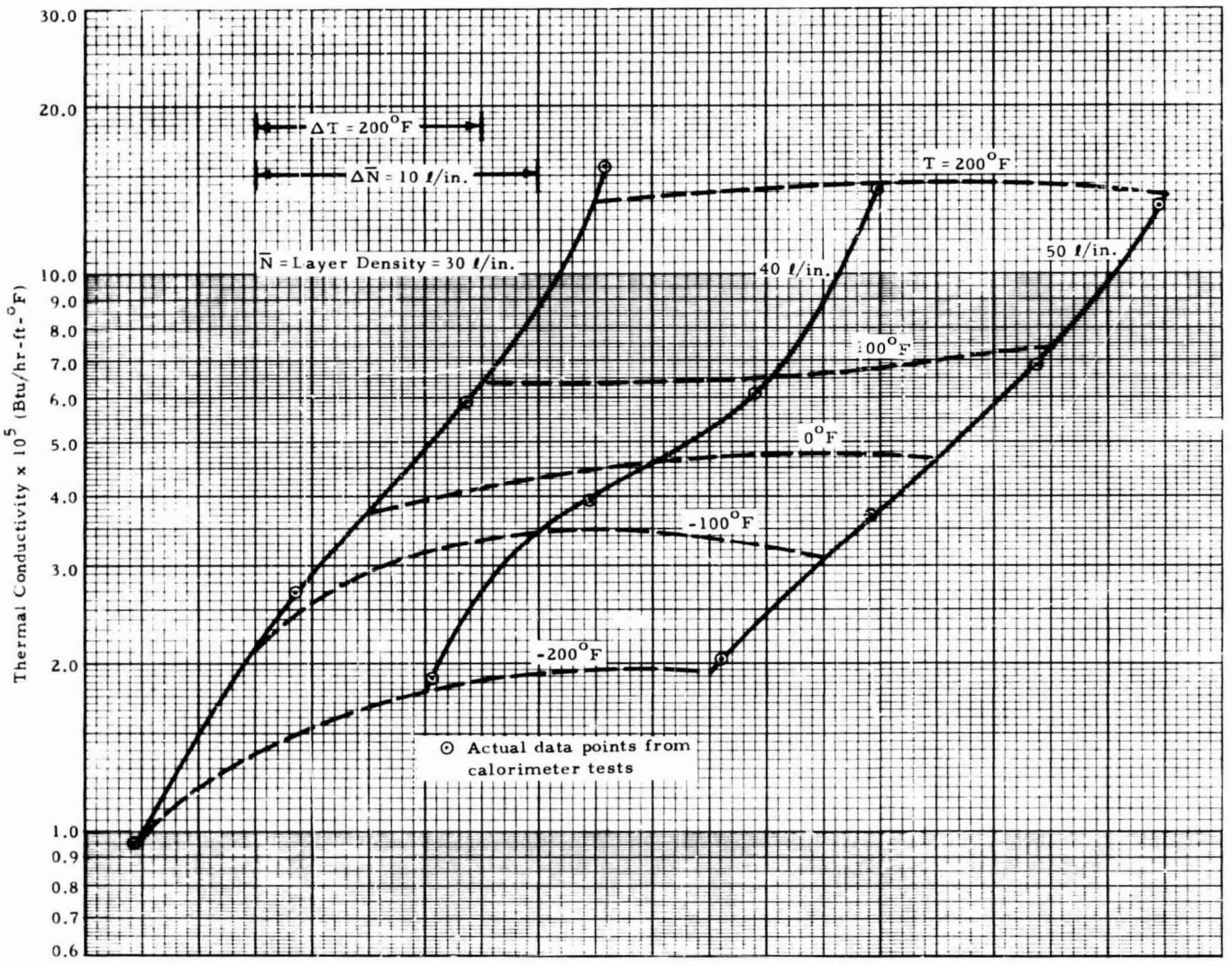

Fig. 10 - Thermal Conductivity Carpet Plot for DAM/GAC-9

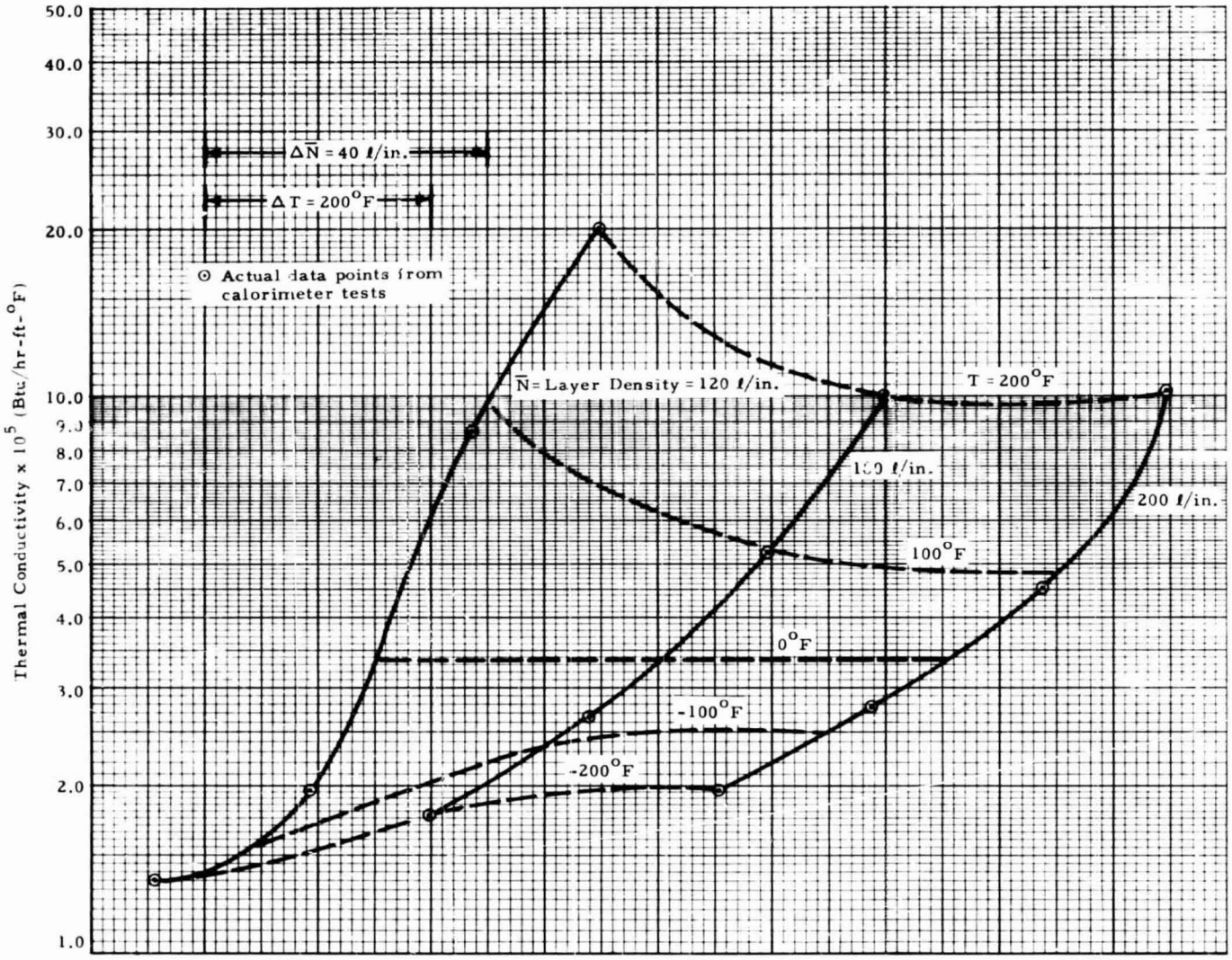

Fig. 11-Thermal Conductivity Carpet Plot for DAM/Dacron Net

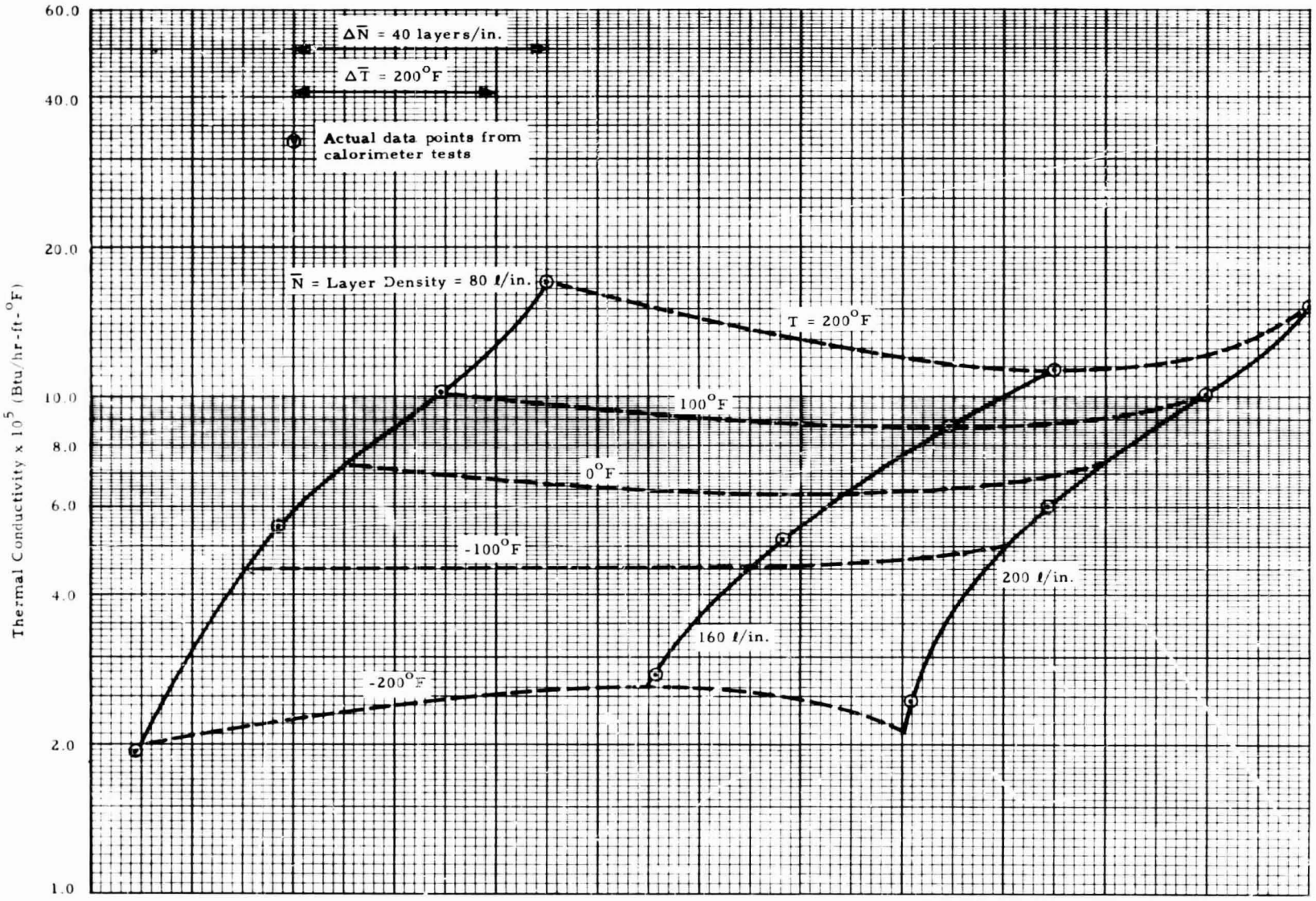

Fig. 12 - Thermal Conductivity Carpet Plot for Superfloc

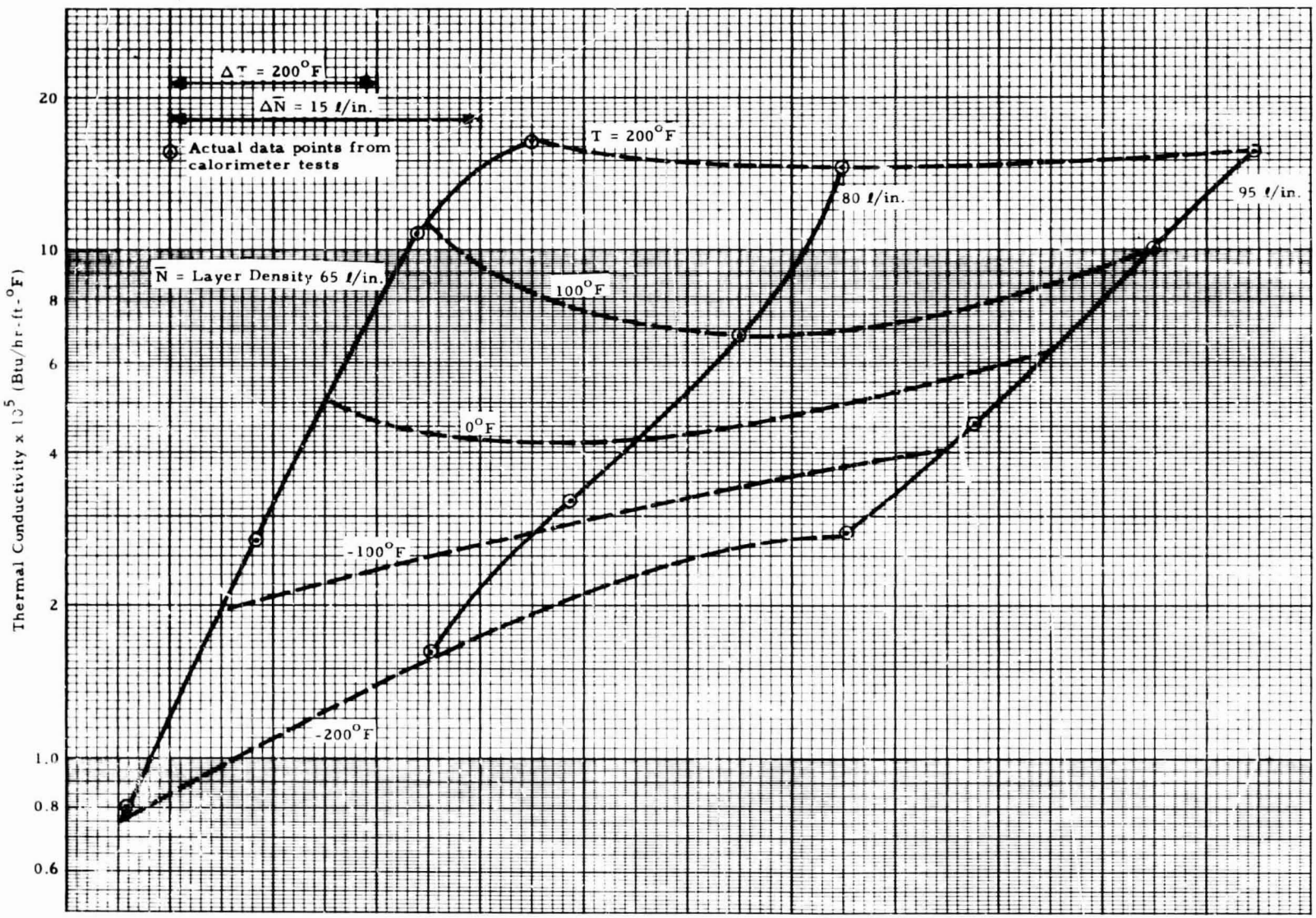

Fig. 13 - Thermal Conductivity Carpet Plot for DAM/Nomex Net

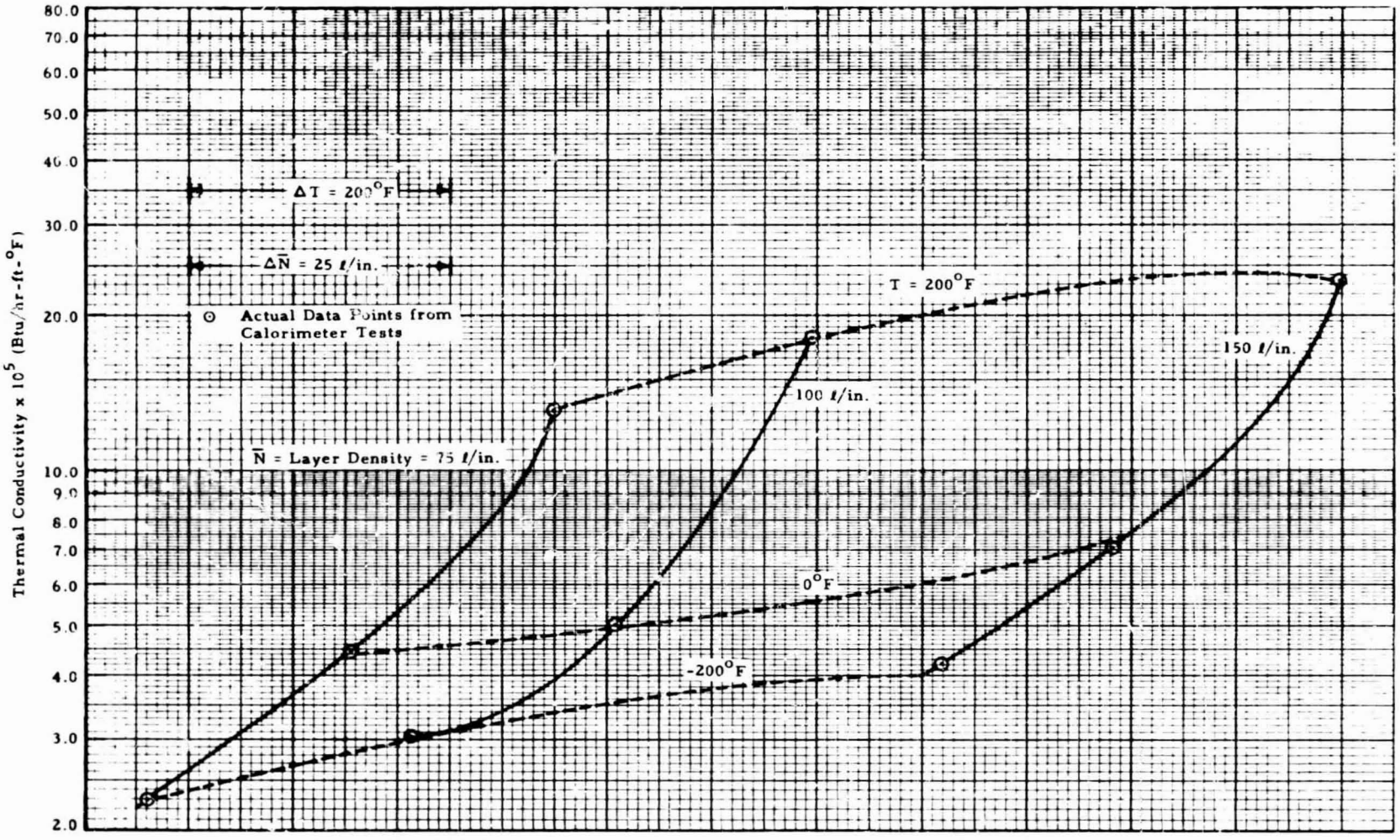

Fig. 14 - Thermal Conductivity Carpet Plot for DAM/Cerex

4.3 DENSITY X THERMAL CONDUCTIVITY DATA FIGURES

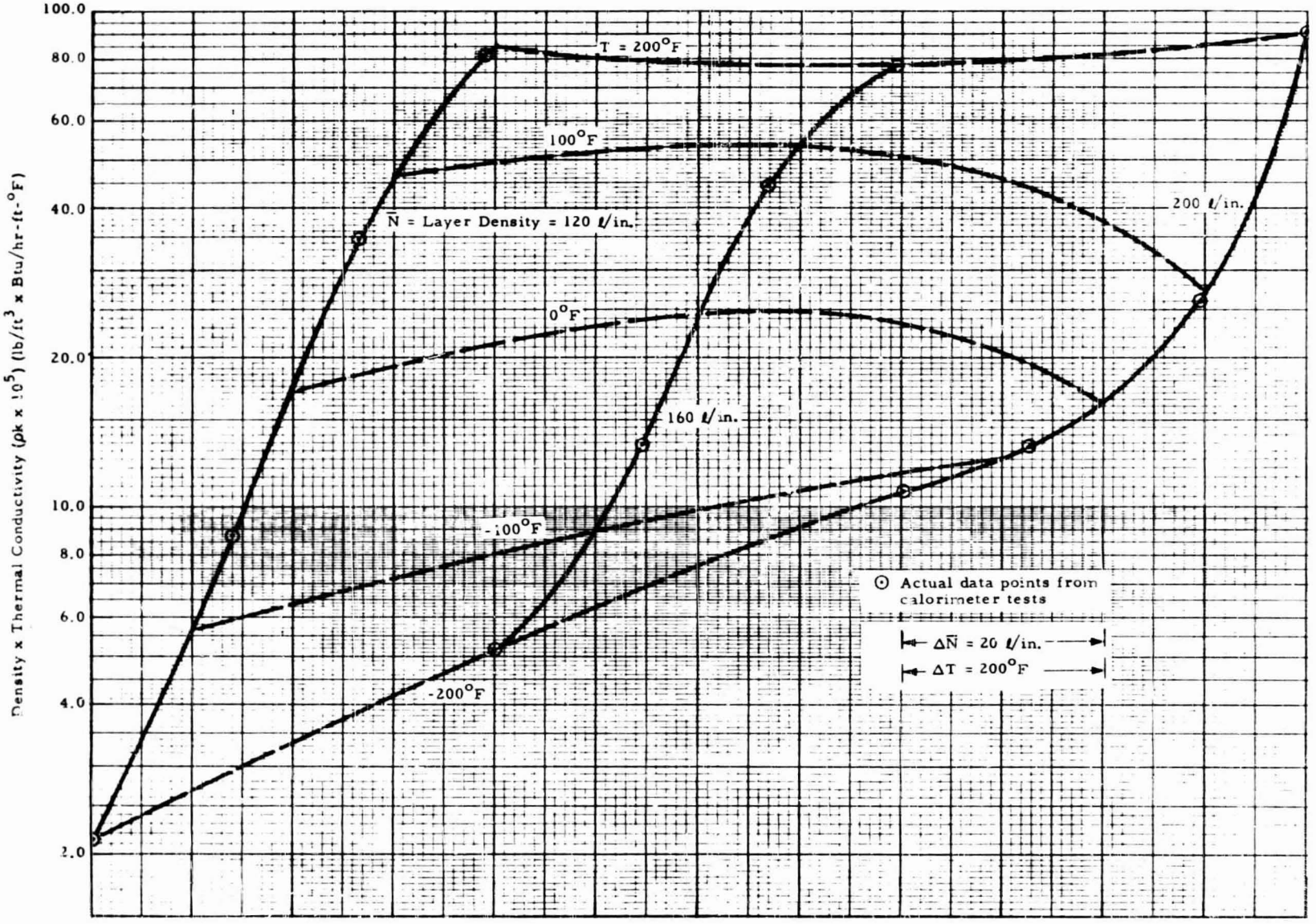

Fig. 15 - Density x Thermal Conductivity Carpet Plot for DAM/Tissuglas

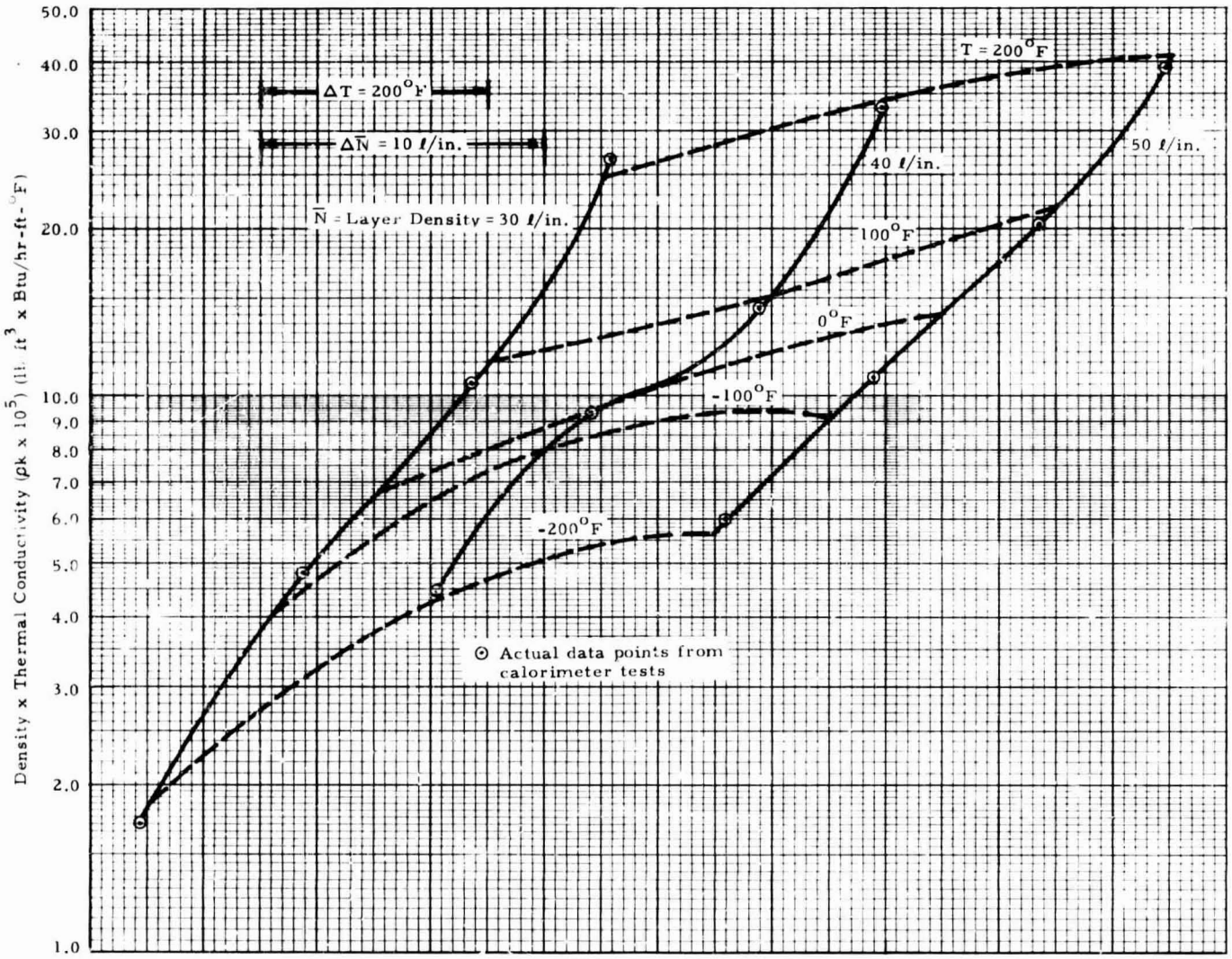

Fig. 16- Density x Thermal Conductivity Carpet Plot for DAM/GAC-9

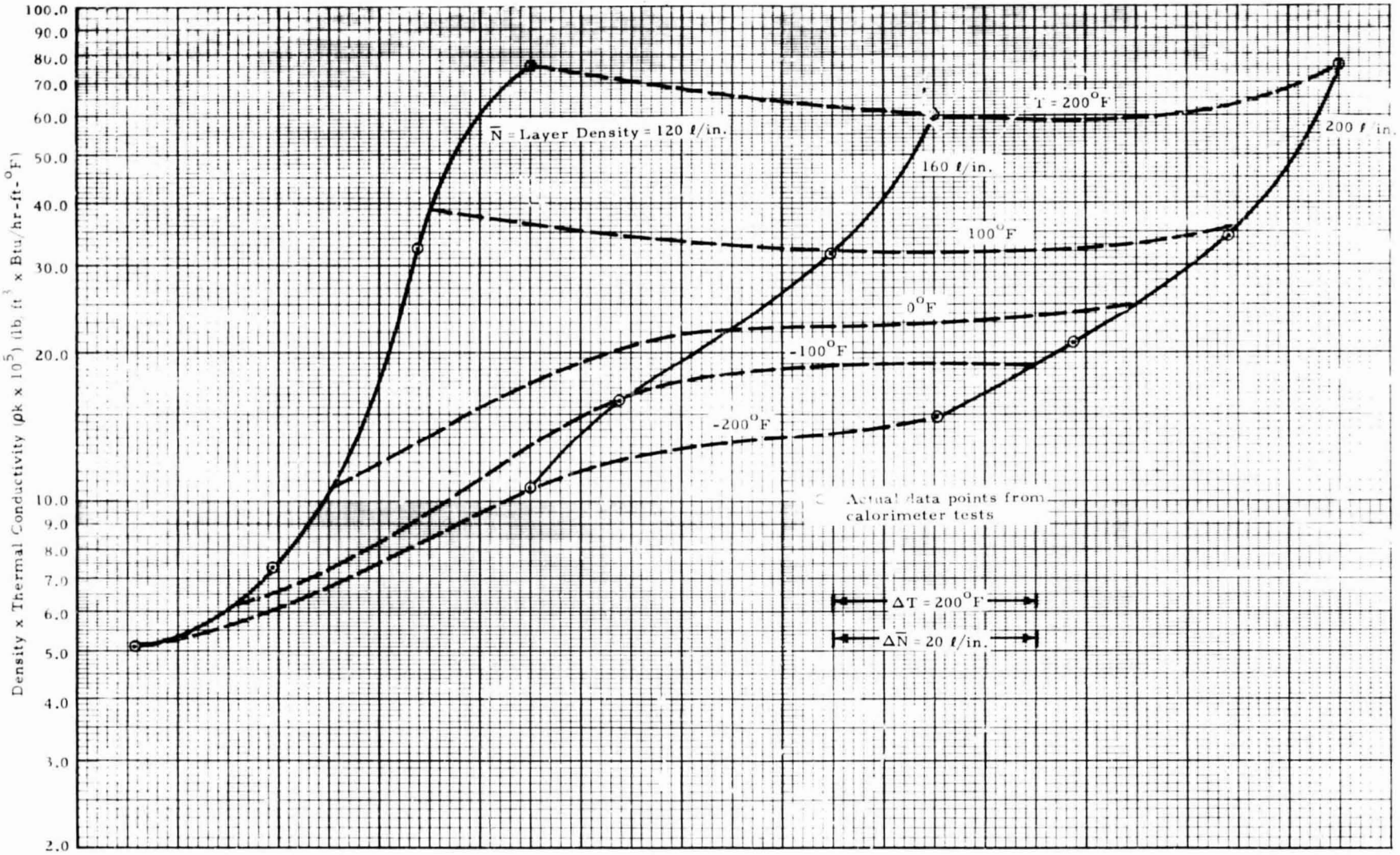

Fig. 17- Density x Thermal Conductivity Carpet Plot for DAM/Dacron Net

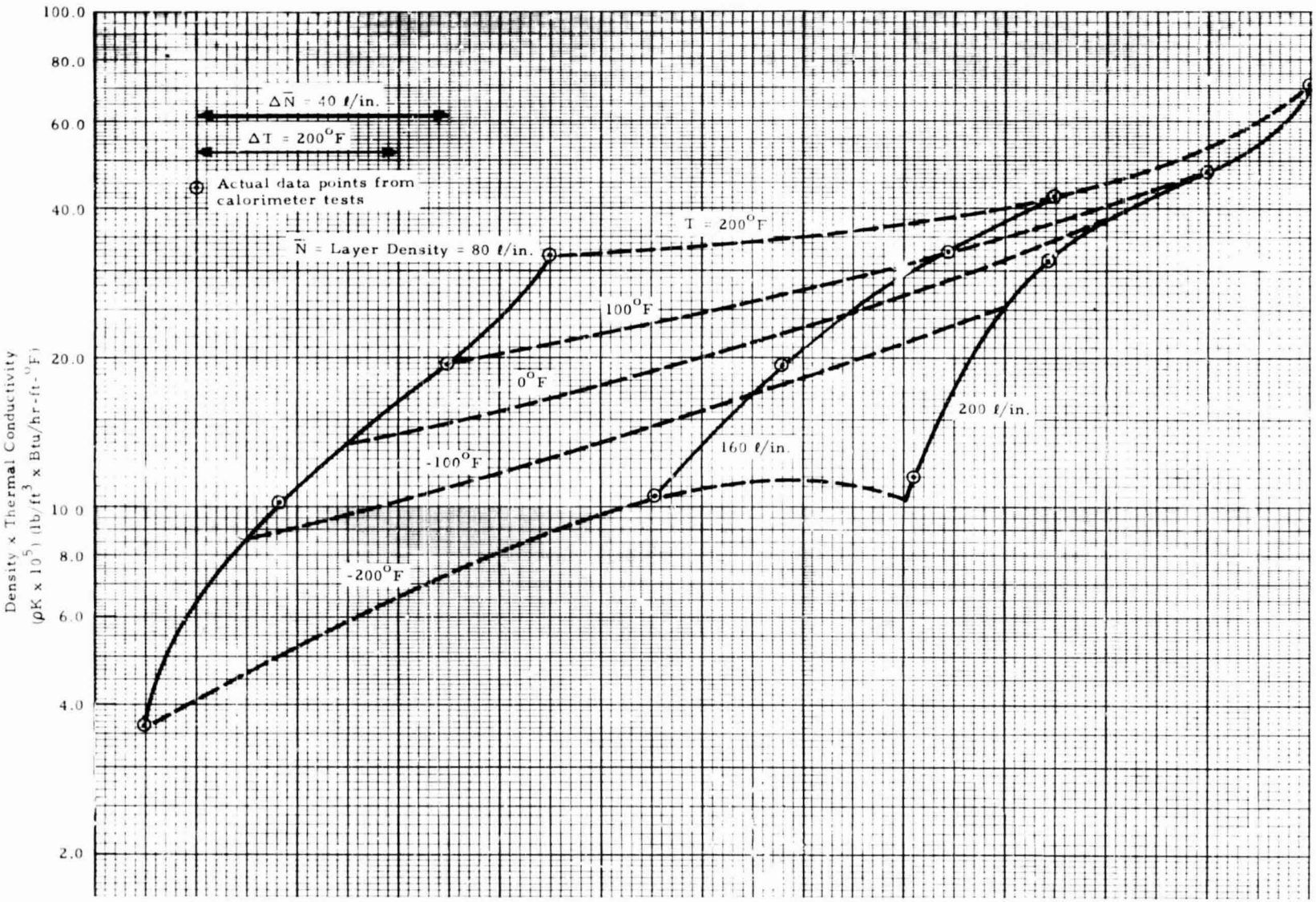

Fig. 18 - Density x Thermal Conductivity Carpet Plot for Superfloc

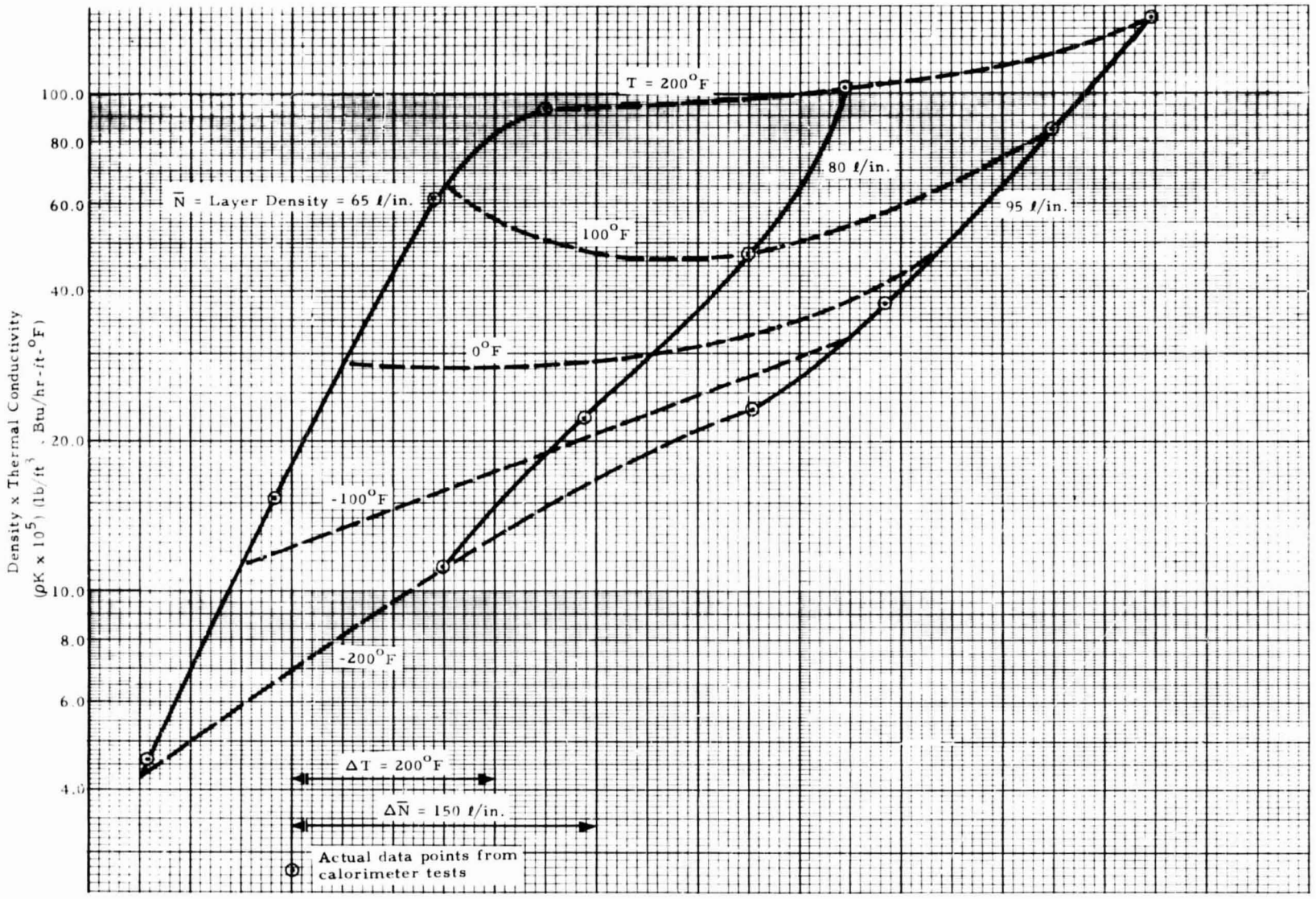

Fig. 19 - Density x Thermal Conductivity Carpet Plot for DAM/Nomex Net

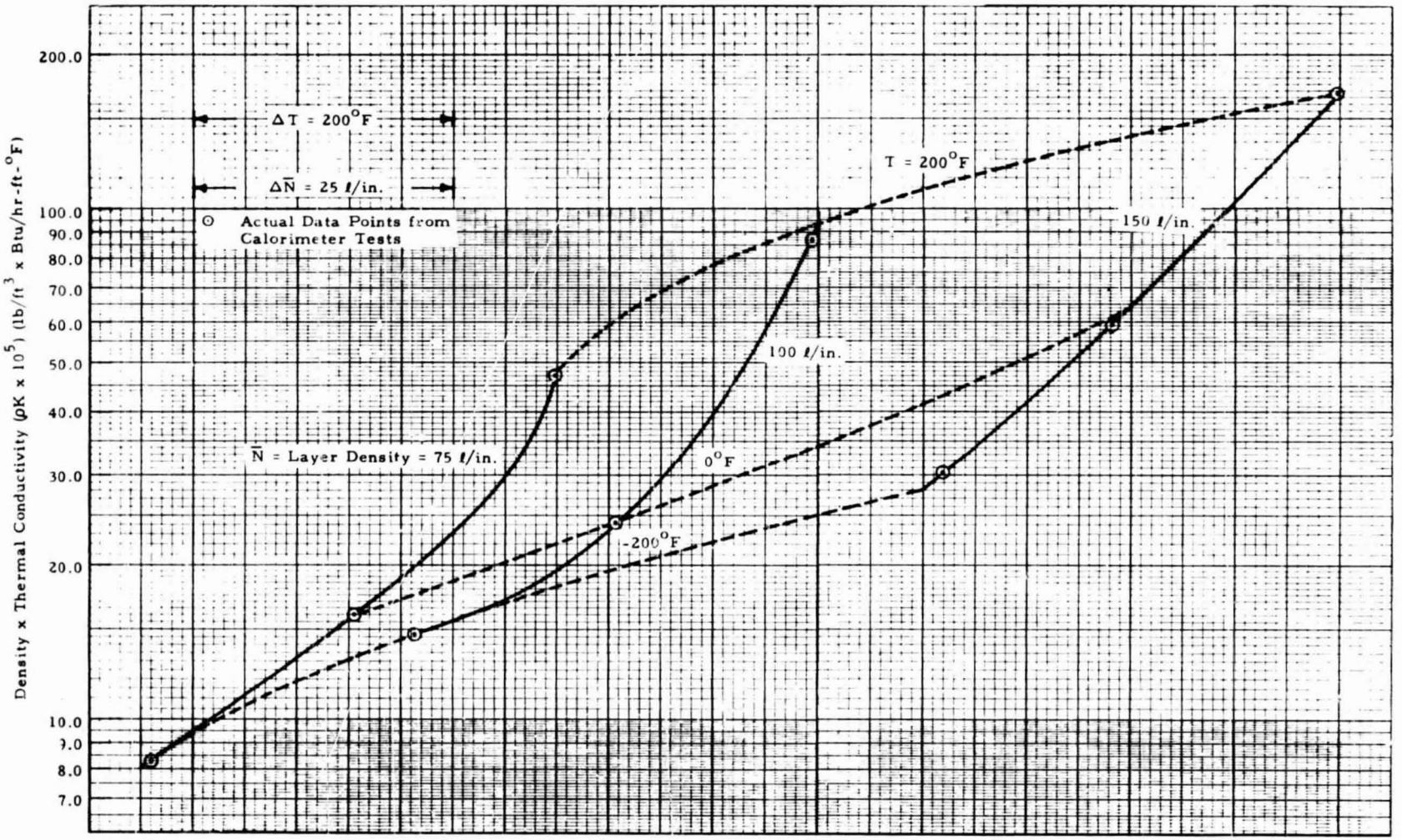

Fig. 20 - Density x Thermal Conductivity Carpet Plot for DAM/Cerex

Section 5
SEMIEMPIRICAL CORRELATION

The semi-empirical correlations represent smooth mathematical surface fits for the empirical data surface and do not exactly fit all data points. These correlations should prove useful for computation and extrapolation, but data interpolated from the carpet plots directly will in general be more accurate, due to the demonstrated accuracy of the data points.

The K and ρK semiempirical correlation for each MLI tested are presented below.

[Units: $T(^{o}R)$, $\bar{N}(\ell/in.)$, $K(Btu/hr\text{-}ft\text{-}^{o}F)$, $\rho(lbm/ft^3)$]

DAM/Tissuglas

$$K \times 10^5 = (1.4271 \times 10^{-5}) \frac{T^3}{\bar{N}} - (2.1744 \times 10^{-2})\, T + (1.8431 \times 10^{-5})\, T^2$$

$$+ (2.2822 \times 10^{-2})\, \bar{N} + (2.2881 \times 10^{-5})\, \bar{N}^2$$

$$\rho K \times 10^5 = [0.0226\, \bar{N} + 0.0212] \left[(1.4271 \times 10^{-5}) \frac{T^3}{\bar{N}} - (2.1744 \times 10^{-2})\, T\right.$$

$$\left. + (1.8431 \times 10^{-5})\, T^2 + (2.2822 \times 10^{-2})\, N + (2.2881 \times 10^{-5})\, \bar{N}^2\right]$$

DAM/GAC-9

$$K \times 10^5 = (5.4307 \times 10^{-7}) \frac{T^3}{\bar{N}} - (3.6901 \times 10^{-2})\, T + (6.3735 \times 10^{-5})\, T^2$$

$$+ (2.7940 \times 10^{-1})\, \bar{N} - (2.7373 \times 10^{-3})\, \bar{N}^2$$

DAM/GAC-9 (Continued)

$$\rho K \times 10^5 = [0.0587\,\overline{N} + 0.0212]\left[(5.4307 \times 10^{-7})\,\frac{T^3}{\overline{N}} - (3.6901 \times 10^{-2})\,T + (6.3735 \times 10^{-5})\,T^2 + (2.7940 \times 10^{-1})\,\overline{N} - (2.7373 \times 10^{-3})\,\overline{N}^{\,2}\right].$$

DAM/Dacron Net

$$K \times 10^5 = (1.1860 \times 10^{-5})\,\frac{T^3}{\overline{N}} - (3.4028 \times 10^{-2})\,T + (1.5993 \times 10^{-5})\,T^2 + (8.9310 \times 10^{-2})\,N - (2.2878 \times 10^{-4})\,N^2$$

$$\rho K \times 10^5 = [0.0377\,N + 0.0212]\left[(1.1860 \times 10^{-5})\,\frac{T^3}{\overline{N}} - (3.4028 \times 10^{-2})\,T + (1.5993 \times 10^{-5})\,T^2 + (8.9310 \times 10^{-2})\,N - (2.2878 \times 10^{-4})\,N^2\right].$$

Superfloc

$$K \times 10^5 = (1.3772 \times 10^{-6})\,\frac{T^3}{\overline{N}} - (1.0014 \times 10^{-1})\,T + (1.3792 \times 10^{-4})\,T^2 + (3.1651 \times 10^{-1})\,\overline{N} - (1.1011 \times 10^{-3})\,\overline{N}^{\,2}$$

$$\rho K \times 10^5 = [0.0236\,\overline{N}]\left[(1.3772 \times 10^{-6})\,\frac{T^3}{\overline{N}} - (1.0014 \times 10^{-1})\,T + (1.3792 \times 10^{-4})\,T^2 + (3.1651 \times 10^{-1})\,\overline{N} - (1.1011 \times 10^{-3})\,\overline{N}^{\,2}\right].$$

DAM/Nomex Net

$$K \times 10^5 = (1.8914 \times 10^{-6})\,\frac{T^3}{\overline{N}} - (6.2879 \times 10^{-2})\,T + (8.9130 \times 10^{-5})\,T^2 + (2.2967 \times 10^{-1})\,\overline{N} - (9.9988 \times 10^{-4})\,\overline{N}^{\,2}$$

DAM/Nomex Net (Continued)

$$\rho K \times 10^5 = [0.0883\,\overline{N} + 0.0212]\left[(1.8914 \times 10^{-6})\,\frac{T^3}{\overline{N}} - (6.2879 \times 10^{-2})\,T + (8.9130 \times 10^{-5})\,T^2 + (2.2967 \times 10^{-1})\,\overline{N} - (9.9988 \times 10^{-4})\,\overline{N}^2\right].$$

DAM/Cerex

$$K \times 10^5 = -(4.5381 \times 10^{-6})\,\frac{T^3}{\overline{N}} - (2.4846 \times 10^{-1})\,T + (3.4207 \times 10^{-4})\,T^2 + (8.9944 \times 10^{-1})\,\overline{N} - (3.8866 \times 10^{-3})\,\overline{N}^2$$

$$\rho K \times 10^5 = [0.0479\,\overline{N} + 0.0212]\left[-(4.5381 \times 10^{-6})\,\frac{T^3}{\overline{N}} - (2.4846 \times 10^{-1})\,T + (3.4207 \times 10^{-4})\,T^2 + (8.9944 \times 10^{-1})\,\overline{N} - (2.8866 \times 10^{-3})\,\overline{N}^2\right].$$

Appendix A
METHOD OF DOUBLE INTERPOLATION

Appendix A

Given the carpet plot in Fig. A-1, in which ρK is shown as a function of T and $\bar{N}$, double interpolation can be used to obtain the ρK value for any set of T and $\bar{N}$ within the ranges of the plot. As an example, if it is desired to determine ρK for $\bar{N}$ = 140 ℓ/in. and T = -50°F, the following method should be used.

1. First, construct the $\bar{N}$ = 140 ℓ/in. curve. This is done by starting at intersection A. From the indicated scale, four large horizontal spaces represents 20 ℓ/in. Therefore, by moving to the right on curve AD a horizontal distance of four spaces, point 1 is located. The coordinates of point 1 are therefore (140 ℓ/in., -100°F). Similarly, starting at intersection B and traveling along curve BC four horizontal spaces to the right locates point 2. The coordinates of point 2 are therefore (140 ℓ/in., 0°F). A curve can now be faired through points 1 and 2 which should parallel AB and CD. This curve represents $\bar{N}$ = 140 ℓ/in.
2. Next, construct the T = -50°F curve. This is done by starting at intersection A. From the indicated scale, one large horizontal space represents 50°F. Therefore, by moving to the right on curve AB a horizontal distance of one space, point 3 is located. The coordinates of point 3 are therefore (120 ℓ/in., -50°F). Similarly, starting at intersection D and traveling along curve DC one horizontal space to the right locates point 4. The coordinates of point 4 are therefore (160 ℓ/in., -50°F). A curve can now be faired through points 3 and 4 which should parallel AD and BC. This curve represents T = -50°F.
3. The intersection (point 5) of curves 1-2 and 3-4 has the desired coordinates (140 ℓ-in., -50°F). The ρK value corresponding to this point can now be read directly from the abscissa, yielding the value:

$$\rho K = 12.5 \times 10^{-5} \text{ (lb/ft}^3\text{)} \times \text{(Btu/hr-ft-}^\circ\text{F)}.$$

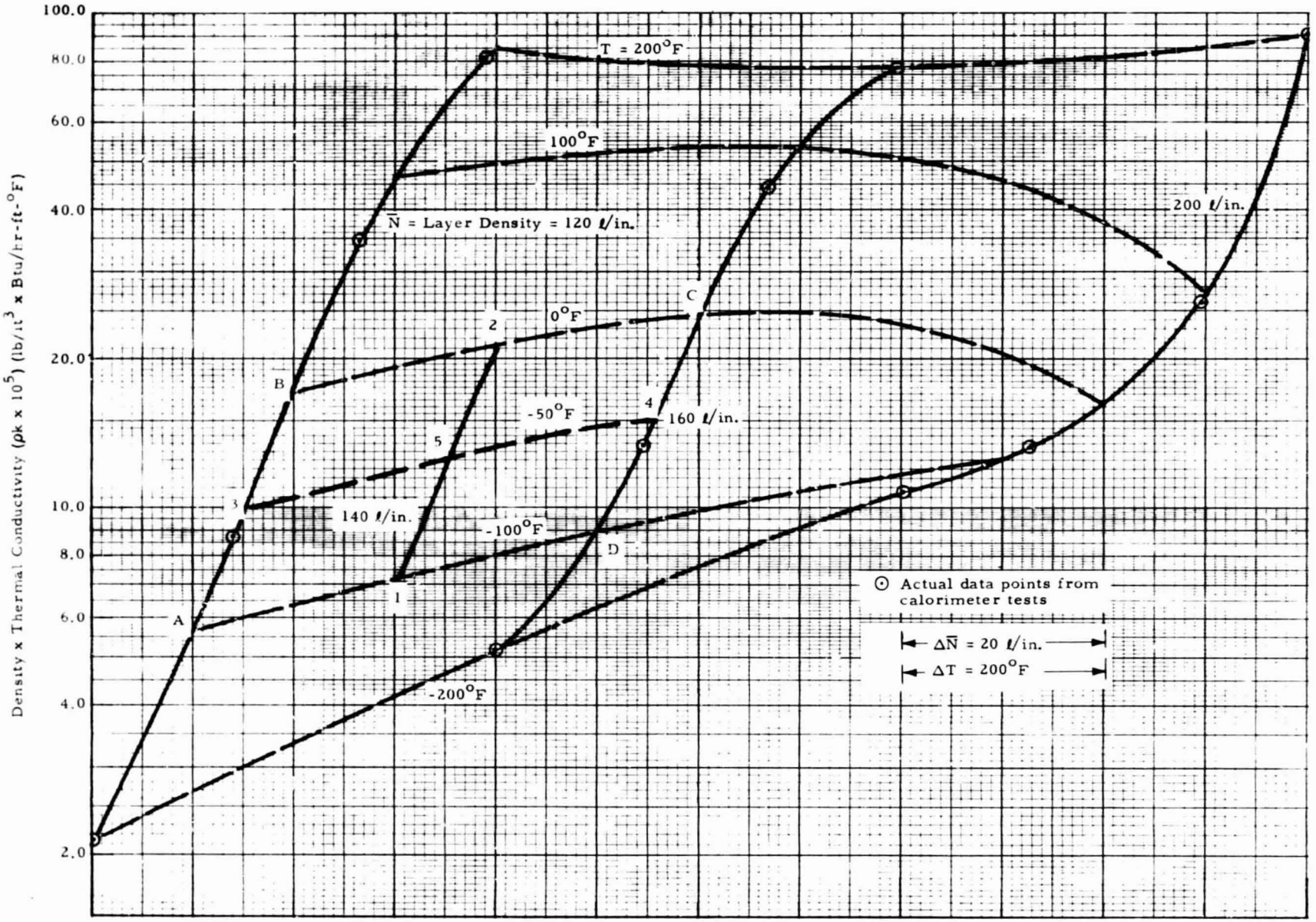

Fig. A-1 - Method for Double Interpolation on Carpet Plot